Stored Energy, Transmission Group Delay and Mode Field Distortion in Optical Fibers

Zoltán Várallyay and Róbert Szipőcs

***Abstract*—The relationship between transmission group delay and stored energy in optical fibers is discussed. We show by numerical computations that the group delay of an optical pulse of finite bandwidth transmitted through a piece of a low loss optical fiber of unit length is proportional to the energy stored by the standing wave electromagnetic field. The stored energy-group delay ratio typically approaches unity as the confinement loss converges to zero. In case of a dispersion tailored Bragg fiber, we found that the stored energy-group delay ratio decreased while the confinement loss increased compared to those of the standard quarter-wave Bragg fiber configuration. Furthermore, a rapid variation in the group delay versus wavelength function due to mode-crossing events (in hollow core photonic bandgap fibers for instance) or resonances originating from slightly coupled cavities, surface or leaking modes in index guiding, photonic bandgap, or photonic crystal fibers always results in a rapid change in the mode-field distribution, which seriously affects splicing losses and focusability of the transmitted laser beam. All of these factors must be taken into consideration during the design of dispersion tailored fibers for different applications.**

***Index Terms*—Optical fiber theory, ultrafast optics, microscopy.**

I. Introduction

DISPERSIVE properties of optical fibers play an important role in long distance, high speed optical data transmission systems [1] and in ultrashort (ps or fs) pulse optical fiber laser systems [2]. When optical fibers are designed for dispersion compensation in optical telecommunication systems, there are a few tradeoffs encountered during their design: they can be designed for a high figure of merit (FOM) or a high dispersion slope for instance the latter one being limited by the required minimum bandwidth or acceptable loss of the fiber for instance [1]. In order to minimize the loss in an optical telecommunication system, one can define the FOM for dispersion compensating fibers (DCF) as the ratio of the negative dispersion coefficient ($\mathbf{D}_{\rm DCF}$) and loss of the DCF module ($\alpha_{\rm DCF}$) [1].

Recently, we have shown [3] that reversed slope ($S < 0$) or flat ($S = 0$), anomalous ($D > 0$), or zero ($D = 0$) dispersion functions can be obtained in a wide wavelength range by introducing resonant structures in the fiber cladding in hollow-core, air-silica photonic bandgap (PBG) fibers or in solid core Bragg fibers with step-index profile. Such optical fibers could be well suited for distortion free delivery or high quality pulse compression of broadly tunable or broadband femtosecond laser pulses in all fiber laser systems, such as femtosecond pulse, all-fiber laser oscillators [2], and amplifiers [4] being suitable for nonlinear microscopy. During the last few years, novel, all-fiber, multimodal (TPF + SHG + CARS) microscope systems have been presented [5]–[7] that can be combined with endoscopy [7], which would greatly increase the utility of nonlinear microscopy for pre-clinical applications and tissue imaging [8]. Application of DCF for pulse shortening, however, might be limited by splicing losses in all fiber laser systems, or by mode-field distortions limiting the focusability of the laser beam exiting the optical fiber delivery and pulse compression system. The focused beam spot size is of primary importance in *in vivo* nonlinear microscopic imaging systems, since the highest signal level must be obtained at a minimal thermal load (absorbed average power level) in order to minimize the risk of thermal damage of the biological sample. Accordingly, when designing optical fibers for nonlinear microendoscopy, not only dispersive and nonlinear properties but mode-field distortions of the dispersion tailored fibers must also be considered. (In contrast to optical telecommunication systems, losses in these fibers are not of primary importance in most practical cases.)

In this paper, we discuss the physics behind the operation of "dispersive" optical fibers, i.e., optical fibers designed for dispersion (D) or dispersion slope (S) compensation to the second- or third-order.

In the followings, we show that the group delay (τ) of a relatively narrowband optical pulse transmitted through a piece of optical fiber of unit length is proportional to the energy stored by the standing wave electromagnetic field at the same (central) frequency, as long as the confinement loss is small. This strong relationship between these two physical quantities is not surprising at all, but has not been emphasized and used for the design of "dispersive" optical fibers. Having this relationship in mind, one can construct higher performance "dispersive" optical fibers, such as high-order mode (HOM) fibers [9], and hollow- or solid-core PBG fibers [3].

In the last section of this paper, we address the question how much the focusability of the laser beam is affected by the superimposed cladding modes present in "dispersive" optical fibers that might be a critical issue in nonlinear microendoscope systems.

II. Theory

There are two basic approaches for tailoring the dispersion of optical waveguide devices: modulating their refractive index profile along the light propagation direction or in the

Manuscript received December 1, 2013; revised February 24, 2014, March 20, 2014, and April 20, 2014; accepted April 20, 2014. This work was supported by the National Development Agency of Hungary under Grant TECH-09-A2-2009-0134 and also by OTKA under Contract 76404.

The authors are with the Institute for Solid State Physics and Optics, Wigner Research Centre for Physics, Hungarian Academy of Sciences, Budapest, Hungary (e-mail: varallyay@szfki.hu; szipocs.robert@wigner.mta.hu).

Color version of one or more of the figures in this paper are available online at http://ieeexplore.ieee.org.

Digital Object Identifier 10.1109/JSTQE.2014.2325394

perpendicular direction. A fiber Bragg grating [10] is one of the most common implementation of the former approach, while dispersion compensation [1] and OmniGuide fibers [11] can be mentioned as typical examples for the latter case. In both cases, changes of the dispersion functions relative to the unperturbed structures have been explained and described, respectively, by the effect of Fabry–Perot type resonances along the direction of propagation [12] or by the effect of cladding modes localized within intentional defects (e.g., Fabry–Perot cavities) in the multilayer cladding [11]. Ghiringhelli and Zervas [12] discussed in detail the relationship between electromagnetic energy density distribution inside the scatterer (i.e., Bragg grating) and the propagation delay in the fiber Bragg grating. A few years later, similar studies were presented by Winful in case of multilayer dielectric mirror structures [13]. Winful analytically showed proportionality between the energy stored in multilayer structure and the so-called dwell time, which is the weighted sum of the reflection group delay and the transmission group delay.

Summarizing the results of [13], we can say that the group delay in a dielectric structure can be related to the stored energy using the Poynting's theorem

$$-\oint_s S\hat{n}\,\mathrm{da} = \frac{\mathrm{dU}}{\mathrm{dt}} \tag{1}$$

where *U* is the electromagnetic field energy and ***S*** is the Poynting vector. Evaluating the surface integral in (1) yields the ratio between the energy and group-delay as shown in Ref. [13]:

$$\mathrm{R}\tau_r + \mathrm{T}\tau_t = \frac{U}{P_i} \tag{2}$$

where P_{i} is the incident power to a dielectric surface, *R* and *T* are the reflection and transmission coefficients ($R + T = 1$), and τ_{r} and τ_{t} are group delays on reflection and transmission, respectively. Numerical simulations in 1-D PBG structures were carried out [14] indicating that the reflection group delay is proportional to the stored energy if the incident power is constant and the transmission of the mirror is negligible: $\tau_{\mathrm{r}} \propto \mathrm{U}$.

In the followings, we check this theory for both PBG and index guiding fibers by a few numerical examples. We derive the dispersion as well as the energy versus wavelength functions for each fiber structure at those wavelength regions where the loss of the fiber is relatively small, i.e., where reflection from the cladding is close to unity.

For calculating the group delay for transmission over the unit length of the fiber, we obtain the effective refractive index (n_{eff}) as the eigenvalue of the Helmholtz equation by evaluating the LP_{01} mode at different wavelengths in the optical fibers.

For our studies, we calculate the transmission group delay for a piece of optical fiber as follows:

$$\tau = \frac{\mathrm{d}\phi}{\mathrm{d}\omega} = \frac{d}{\mathrm{d}\omega}\left(\frac{\omega \mathrm{L}}{c} n_{\mathrm{eff}}(\omega)\right) \tag{3}$$

where $n_{\mathrm{eff}}(\omega)$ and *L* are the frequency dependent effective refractive index and the length of the fiber, respectively.

The stored energy (*U*) in a piece of the fiber with length *L* can be derived from the electric and magnetic field distributions (eigenfunctions) we obtain from the Helmholtz eigenvalue equation as follows:

$$\begin{aligned}\mathrm{U} &= \iiint u\; dV = \iiint \left(\frac{1}{2}\varepsilon E^2 + \frac{1}{2}\mu H^2\right) dV \\ &= \frac{L}{2}\iint \left(\varepsilon_o n^2 E^2 + \mu_o H^2\right) dA\end{aligned} \tag{4}$$

where the simplification in the integral results from the longitudinal uniformity (*E* and *H* are independent of the *z* coordinate) and $\mu_r = 1$. The normalization of the modes at different frequencies were done by choosing

$$\frac{1}{2}\iint (\vec{E} \times \vec{H})\vec{u}_z dA = 1 \tag{5}$$

where $\vec{u}_z$ is the unit vector in the axial (*z*) direction. Note that this normalization procedure assures that the incident power (P_i) is unity for the different frequencies. Therefore, the U/τ quotient should be equal to one in the loss-less case as explained earlier in this section.

III. Numerical Results

In this section, we investigate five different fiber structures by numerical simulations, three of them are PBG fibers and two of them are index guiding fibers.

In order to check the effect of a finite, frequency dependent, non-zero confinement loss in optical fibers, we perform simulations for solid core PBG fibers of two different kinds: a regular Bragg fiber with circular, alternating high, and low index regions around the core, which has the same refractive index than the low index layers and a similar Bragg fiber with an additional resonant layer around the core [3]. The low index layers in the investigated fiber structures are made of fused silica, while the refractive index of the high index layers is higher by 0.015 than that of the low index layer at the entire wavelength range we investigate. The core radius of the fiber is $R_c = 8\ \mu$m and the thicknesses of the alternating high and low index layers are $d_H = 1.4\ \mu$m and $d_L = 4.9\ \mu$m, respectively. The number of HL periods in the cladding region is seven. One of the designs has a standard quarterwave-stack structure, while another has a resonant layer around the core in order to minimize the dispersion slope at around 1 μm [3]. The resonant layer a has refractive index difference of 0.008 relative to fused silica and a physical thickness of 1.6 μm. The bandgaps of both Bragg fibers are in the 700–1500 nm wavelength range. The third PBG fiber is a hollow-core fiber having a photonic-crystal cladding with a hexagonal rotational symmetry. This fiber is a HC-1060 type fiber (NKT Photonics, Denmark), which has a bandgap between 1 and 1.1 μm. The geometrical parameters we use at this fiber are the followings: six periods are calculated around the core, the pitch is $\Lambda = 2.82\ \mu$m, and the hole size is $d = 2.746\ \mu$m. The holes around the core form a honey-comb structure where the holes possess hexagonal shapes with rounded corners. The diameter of the rounding circle is $d_c = 0.66\ \mu$m and directly around the core some pentagonal shapes appear, which have a rounding at the 90° edge of $d_p = 0.16\ \mu$m.

The index guiding fibers are of two kinds: a standard, low confinement loss single mode fiber designed to operate around

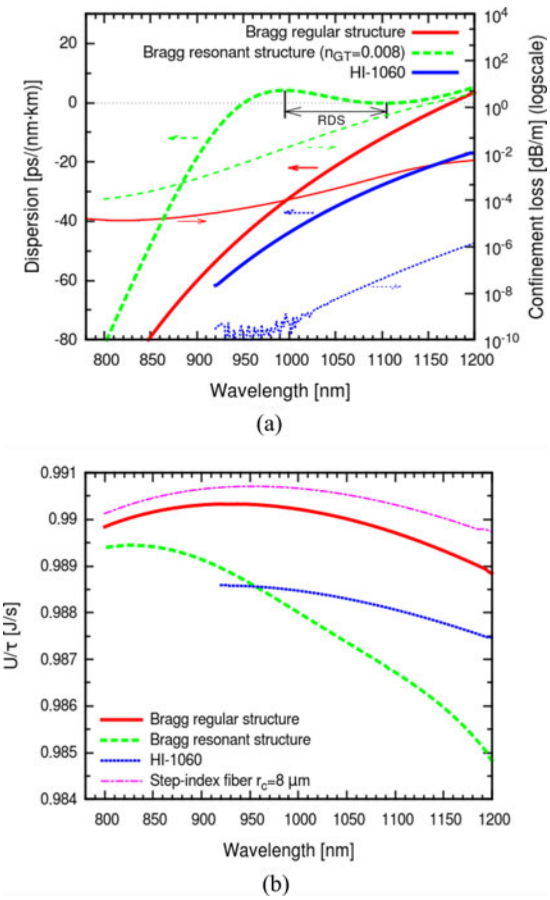

Fig. 1. (a) Computed dispersion versus wavelength functions (thick lines), corresponding confinement losses (thin lines) and (b) computed stored energy-group delay ratio (U/τ) versus wavelength functions of solid core PBG fibers of two different designs and of two different index-guiding fibers. One of the index guiding fibers is similar to HI-1060 of Corning, while the second one has an 8 μm core radius. Each fiber has a unit length of 1 m and the incident power is 1 W.

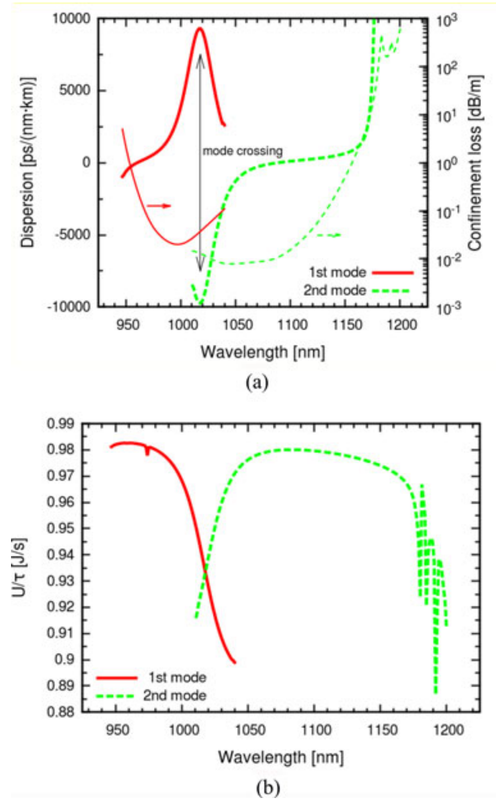

Fig. 2. (a) Dispersion versus wavelength functions (thick lines), corresponding confinement loss values (thin lines) computed for the two fundamental modes in the HC-1060 type fiber and (b) computed U/τ ratios for the two modes. Long wavelength edge of the first mode bandgap and the short wavelength edge of the second mode bandgap can be observed in the dispersion versus wavelength functions as well as in the U/τ curves at wavelengths where the U/τ value drops quickly (at around 1020 nm).

one micrometer: it is a HI-1060 type fiber from Corning. In our simulations, we used refractive index data of fused silica for the cladding by using the corresponding Sellmeier formula, while the refractive index difference between the core and the cladding was kept constant $\Delta n = 0.0075$ over the 920–1200 nm range. The core diameter is $d_{\rm core} = 5.3\ \mu$m. The second kind of index guiding fiber is a large mode area (LMA) fiber having a 16 μm core diameter and the same index difference that was used in the case of HI-1060 type fiber.

A. Dispersion, Loss, and Stored Energy

The computed dispersions and confinement losses for the two Bragg fibers and the HI-1060 fiber are shown in Fig. 1(a), while the ratio between the stored energy and the group delay is depicted in Fig. 1(b) for all of the fibers. The dispersion and loss of the LMA fiber is approximately the same as the HI-1060 type, therefore, we have not added these curves to Fig. 1(a). The dispersion of LMA runs with a few ps/(nm·km) above the dispersion of HI-1060 fiber and the loss of the large core fiber is somewhat smaller than the loss of HI-1060. In Fig. 1(b), it can be clearly seen that the ratio is very close to unity all over the fiber transmission band, furthermore, the lower confinement loss increases the energy-group delay ratio. The relatively low U/τ ratio of the HI-1060 fiber can be explained by its small core size compared to the rest of the fibers we investigated. We also evaluated the dispersion and loss properties of the HC-1060 type, hollow-core fiber model and the U/τ ratio the results of which are shown in Fig. 2(a) and (b), respectively.

The index-guiding fiber has a significantly lower loss than the HC-1060 type fiber [see Fig. 1(a)], therefore, we may expect a lower U/τ ratio for the HC-1060 fiber, which is confirmed by Fig. 2(b) where the U/τ ratio remains below the value of 0.98 even in the center of the bandgap. This number is close to 0.99 in case of HI-1060 fiber for all over the investigated wavelength range. In the case of the HC-1060 fiber, we found a leaking mode (mode crossing between two modes) at around 1025 nm, therefore, the first and the second modes are calculated, and respectively, plotted in the dispersion function [see Fig. 2(a)] and in the U/τ graph [see Fig. 2(b)] below and above this specific wavelength. The latter plot shows a large variation of the energy-group delay ratio from the center to the edge of the two bandgaps.

In Fig. 3, we show two examples of how the U/τ delay ratio approaches unity as the confinement loss converges to zero in

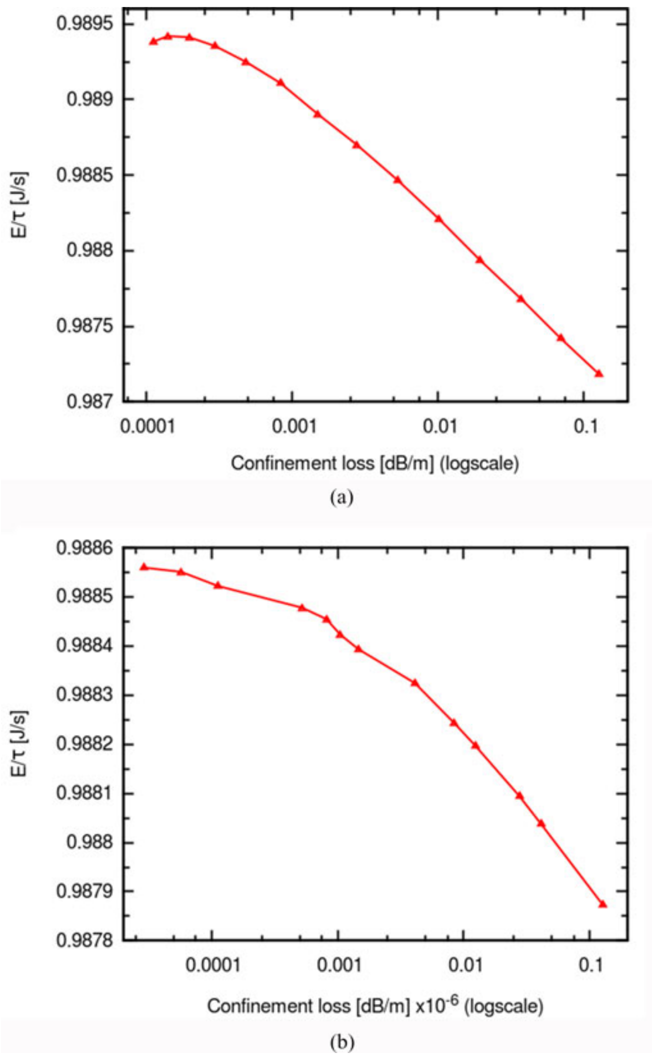

Fig. 3 E/τ ratio as a function of the confinement loss computed for the (a) solid core Bragg fiber with an additional resonant (GT) layer around the core and for the (b) HI-1060 fiber.

case of the solid core Bragg fiber with an additional resonant (GT) layer around the core [see Fig. 3(a)] and for the step-index HI-1060 SM fiber [see Fig. 3(b)]. Interestingly, such a one-to-one correspondence between the U/τ delay ratio and the confinement loss could not be confirmed by our simulations in case of the solid core Bragg fiber without the resonant layer around the core, a fact that needs further investigations. Note that a similar discrepancy has been reported in Ref. [14] dealing with 1-D dispersive PBG structures.

In order to understand the relationship between mode profile variations and the dispersive properties of the fiber, we display a few fundamental core mode profiles at different wavelengths in case of the HC-1060 fiber in Fig. 4. The leaking mode range at around 1025 nm can be clearly seen in Fig. 4(c), where a significant portion of the energy propagates in the glass region of the cladding. This behavior causes a large variation in the dispersion functions at around 1025 nm [see Fig. 2(a)] and results in a large positive or negative chirp on ultrashort pulses centered at around 1025 nm. Accordingly, such optical pulses may suffer significant temporal and spatial distortions during their propagation in this wavelength regime. Due to increased scattering and transmission losses, we can also observe a drop in the U/τ ratio [see Fig. 2(b)].

B. Focusability of the Distorted Modes

If one modifies the dispersion of an optical fiber by structural modifications that results in some resonant behavior, the propagating fundamental mode profile will be distorted relative to the original fiber cross-section geometry. Note, that similar distortions can be observed in the case of leaking modes or surface modes appearing in hollow core PBG fibers, as shown in Fig. 4. In that case, the regular hexagonal geometry of the HC-1060 fiber was not modified by purpose, but the appearing leaking mode (or mode crossing event) at around 1025 nm resulted in a large variation in the dispersion profile [see Fig. 2(a)] as well as a highly distorted fundamental mode profile [Fig. 4(c)].

The question arises: how well the distorted modes of dispersive fibers can be applied, for example, for two photon microscopy, where focusability of the fiber delivered ultrashort pulses is of primary importance [4]. In order to investigate this question, we calculate the intensity square of the mode field distribution in the Fourier space, which can be related to the effectiveness of the two-photon absorption or second harmonic generation in the focal plane of a focusing element, such as a microscope objective. Therefore, we compute the following ratio for the computed mode field distributions at each wavelength

$$\rho(\lambda) = \frac{\int_0^k \int_0^{2\pi} \tilde{I}(k_r, k_\varnothing, \lambda)^2 dk_\varnothing dk_r}{\int_0^k \int_0^{2\pi} \tilde{I}_0(k_r, k_\varnothing, \lambda)^2 dk_\varnothing dk_r} \tag{6}$$

where $\tilde{I}\,(k_r, k_\phi, \lambda)$ is the 2-D Fourier transform of the intensity distribution of an arbitrary mode profile at wavelength λ, and $\widetilde{I_0}\,(k_r, k_\phi, \lambda)$ is the Fourier transform of the "ideal" mode profile, which is obtained by filtering out the higher spatial frequencies from $\tilde{I}\,(k_r, k_\phi, \lambda)$. In this way, we can neglect the effect of rapid mode size variations with wavelength at resonances.

The obtained $\rho(\lambda)$ functions for the HC-1060 type and the reversed dispersion slope Bragg fibers are shown in Fig. 5. The figure clearly shows that in case of a commercial HC-1060 fiber, we lose approximately 10% of the power for two-photon absorption or second-harmonic generation due to mode-field distortion. The fact is that the mode partially propagates in the cladding, which results in some deviation from a first order Bessel function that would be the ideal excitation mode profile for focusing. At wavelengths where the surface modes are more enhanced, the focusability of the mode drops down to ~25%. According to Fig. 5, we can say that the propagating modes of this hollow core fiber have a good focusability at 960 and 1100 nm. Of course, the performance of the HC-1060 fiber could be improved by increasing the air–glass ratio in the cladding, i.e., choosing thinner wall thickness [15].

In Fig. 5, we also plotted the $\rho(\lambda)$ function for a resonant Bragg fiber discussed earlier [see Fig. 1(a)]. The reversed dispersion slope profile is obtained at the expense of a modified, resonant fiber mode profile, which resembles an LP_{02} mode

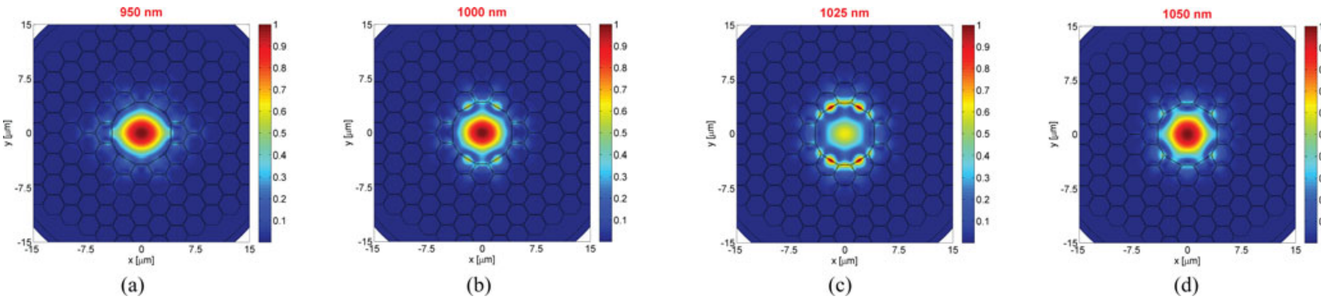

Fig. 4. Fundamental mode profiles in the core of a HC-1060 fiber at (a) 950, (b) 1000, (c) 1025, and (d) 1050 nm. The mode profiles shown in Figs. (a) and (b) correspond to the so-called first mode, while those shown in Figs. (c) and (d) correspond to the second mode.

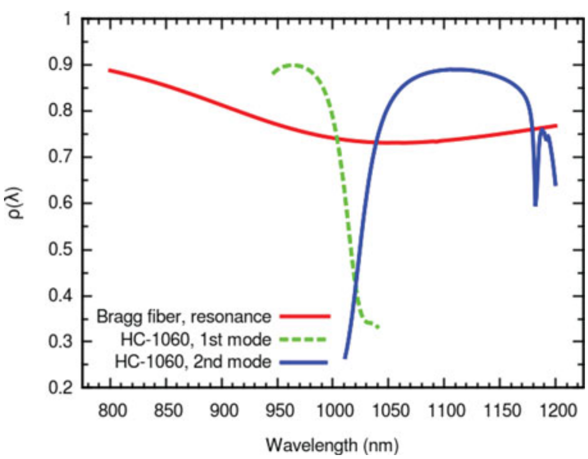

Fig. 5. Focusability $\rho(\lambda)$ of the propagating fundamental modes defined by Eq. (6) and calculated for a reversed dispersion slope, resonant Bragg fiber (red curve) and for a hollow core PBG fiber (green and blue curves) near resonance and leaking mode wavelengths.

field distribution at the resonance wavelengths, since the "tail" of the mode propagates in the resonant layer [16]. Fig. 5 shows that focusability of the fiber mode in this Bragg fiber is also decreasing when reaching the reversed dispersion slope region (975–1100 nm). At around 1050 nm, we lose approximately 30% of the focused beam power and the focusability increases for longer wavelengths.

IV. Summary

We found that the U/τ ratio is very close to unity all over the fiber transmission band, furthermore, the lower confinement loss increases the energy-group delay ratio close to unity [18]. Since the stored energy in the fiber is derived from the electric field distributions at each wavelength [see (4)], we learned that modifications in the dispersion function of any optical fiber always result in a change in the mode field distribution at each wavelength, and vice versa. As a consequence, dispersion tailored optical fibers, such as HOM fibers [9] and hollow- or solid-core PBG fibers [3] having a desired group-delay dispersion functions have a reduced focusability of the collimated laser beam or an increased splicing loss over most of the useful range of operation [3] due to the superimposed cladding modes, which can be a critical issue in fiber integrated nonlinear microendoscope systems for instance. From this relationship, it also follows that surface modes appearing in hollow core PBG fibers seriously affect the dispersion profile of these optical fibers [3].

In connection with telecommunication systems and having in mind that the difference in the group delay over the operation frequency range is nothing else but the integral of the dispersion over the given frequency range, we can say that the previously discussed special parameter U/τ, or FOM along with the corresponding group delay value τ can be also used to characterize the performance of different dispersion compensating optical fibers regarding transmission loss and dispersion for instance [1], [17].

Note added: The rapidly varying group delay versus wavelength functions near resonance or leaking mode wavelengths of different fiber samples can be precisely characterized by state of the art spectral interferometric methods such as the Fourier-transform method discussed in the recent paper of Ref. [19].

References

[1] M. Wandel and P. Kristensen, "Fiber designs for high figure of merit and high slope dispersion compensating fibers," *J. Opt. Fiber Commun. Rep.*, vol. 3, pp. 25–60, 2005.

[2] J. Fekete, A. Cserteg, and R. Szipőcs, "All-fiber, all-normal dispersion ytterbium ring oscillator," *Laser Phys. Lett.*, vol. 6, pp. 49–53, 2009.

[3] Z. Várallyay, K. Saitoh, Á. Szabó, and R. Szipőcs, "Photonic bandgap fibers with resonant structures for tailoring the dispersion," *Opt. Exp.*, vol. 17, pp. 11869–11883, 2009.

[4] A. Kolonics, D. Csáti, P. Antal, and R. Szipőcs, "A simple, cost efficient fiber amplifier wavelength extension unit for broadly tunable, femtosecond pulse Ti-sapphire lasers for CARS microscopy," presented at the Biomedical Optics Congr., Miami, FL, USA, 2012, Paper BSu3A.28.

[5] A. F. Pegoraro, A. Ridsdale, D. J. Moffatt, J. P. Pezacki, B. K. Thomas, L. Fu, L. Dong, M. E. Fermann, and A. Stolow, "All-fiber CARS microscopy of live cells," *Opt. Exp.*, vol. 17, pp. 20701–20706, 2009.

[6] M. Baumgartl, M. Chemnitz, C. Jauregui, T. Meyer, B. Dietzek, J. Popp, J. Limpert, and A. Tünnermann, "All-fiber laser source for CARS microscopy based on fiber optical parametric frequency conversion," *Opt. Exp.*, vol. 20, pp. 4484–4493, Feb. 2012.

[7] B. G. Saar, R. S. Johnston, C.W. Freudiger, X. S. Xie, and E. J. Seibel, "Coherent Raman scanning fiber endoscopy," *Opt. Lett.*, vol. 36, pp. 2396–2398, 2011.

[8] C. W. Freudiger, R. Pfannl, D. A. Orringer, B. G. Saar, M. Ji, Q. Zeng, L. Ottoboni, W. Ying, C. Waeber, J. R. Sims, P. L. De Jager, O. Sagher, M. A. Philbert, X. Xu, S. Kesari, X. S. Xie, and G. S. Young, "Multicolored stain-free histopathology with coherent Raman imaging," *Lab. Invest.*, vol. 92, pp. 1492–1502, Oct. 2012.

[9] S. Ramachandran, S. Ghalmi, J. W. Nicholson, M. F. Yan, P. Wisk, E. Monberg, and F. V. Dimarcello, "Anomalous dispersion in a solid, silica-based fiber," *Opt. Lett.*, vol. 31, pp. 2532–2534, 2006.

[10] K. O. Hill, Y. Fujii, D. C. Johnson, and B. S. Kawasaki, " Photosensitivity in optical fiber waveguides: Application to reflection fiber fabrication," *Appl. Phys. Lett.*, vol. 32, pp. 647–649, 1978.

[11] T. Engeness, M. Ibanescu, S. Johnson, O. Weisberg, M. Skorobogatiy, S. Jacobs, and Y. Fink, "Dispersion tailoring and compensation by modal interactions in OmniGuide fibers," *Opt. Exp.*, vol. 11, pp. 1175–1196, 2003.

[12] F. Ghiringhelli and M. N. Zervas, "Time delay distribution in Bragg gratings," *Phys. Rev. E*, vol. 95, no. 13, pp. 036604-1–036604-13, 2002.

[13] H. G. Winful, "The meaning of group delay in barrier tunnelling: A reexamination of superluminal group velocities," *New J. Phys.*, vol. 8, pp. 101-1–101-16, 2006.

[14] P. G. Antal and R. Szipőcs, "Relationships among group delay, energy storage, and loss in dispersive dielectric mirrors," *Chin. Opt. Lett.*, vol. 10, pp. 053101-1–053101-4, 2012.

[15] T. Murao, K.Saitoh, and M. Koshiba, "Structural optimization of air-guiding photonic bandgap fibers for realizing ultimate low loss waveguides" *J. Lightw. Technol.*, vol. 26, no. 12, pp. 1602–1612, Jun. 2009.

[16] Z. Várallyay, K. Saitoh, J. Fekete, K. Kakihara, M. Koshiba, and R. Szipőcs, "Reversed dispersion slope photonic bandgap fibers for broadband dispersion control in femtosecond fiber lasers," *Opt. Exp.*, vol. 16, pp. 15603–15616, 2008.

[17] A. Carena, V. Curri, G. Bosco, R. Cigliutti, E. Torrengo, P. Poggiolini, A. Nespola, D. Zeolla, and F. Forghieri, "Novel figure of merit to compare fibers in coherent detection systems with uncompensated links," *Opt. Exp.*, vol. 20, pp. 339–346, 2012.

[18] Z. Várallyay, P.G. Antal, and R. Szipőcs, "Relation between transmission group delay and stored energy in optical fibers," presented at the Ultrafast Optics Conf., Davos, Switzerland, Mar. 2–8, 2013, Paper MoP.19.

[19] T. Grósz, A. P. Kovács, M. Kiss, and R. Szipőcs, "Measurement of higher order chromatic dispersion in a photonic bandgap fiber: Comparative study of spectral interferometric methods," *Appl. Opt.*, vol. 53, pp. 1929–1937, 2014.

Zoltán Várallyay was born in Budapest, Hungary, in 1974. He received the M.Sc. degree from the University of Szeged, Szeged, Hungary, in 2001 and the Ph.D. degree from the Budapest University of Technology and Economics, Budapest, Hungary, in 2007, both in Physics.

Since 2000, he has been working for the Furukawa Electric Institute of Technology Ltd., Budapest, Hungary. He has been also a part-time scientist at the Wigner Research Centre for Physics, Hungarian Academy of Sciences, Budapest, since 2008. His current research interests include optical fiber related theoretical problems including nonlinear, ultrashort pulse transmission and compression in conventional and microstructured fibers, amplification in doped and Raman fiber amplifiers, polarization mode dispersion in mechanically stressed optical fibers, and the design of photonic bandgap fibers with tailored dispersive properties.

Róbert Szipőcs was born in Zalaegerszeg, Hungary, in 1964. He received the M.Sc. degree in electrical engineering from the Technical University of Budapest, Budapest, Hungary, in 1987 and the Ph.D. degree in physics from the University of Szeged, Szeged, Hungary, in 2001.

From 1987, he has been working for the Institute for Solid State Physics and Optics, Wigner Research Center for Physics, Hungarian Academy of Sciences, Budapest. From 1997, he is the Managing Director of R&D Ultrafast Lasers Ltd. He is the author of more than 40 articles, and a few patents. His research interests include dispersive properties of optical coatings and fibers, ultrafast solid state and fiber lasers, and nonlinear microscopy. He is a Member of the Optical Society of America. He received the ICO/ICTP Award in 2002 for his fundamental work in development of dispersion compensating mirrors such as chirped mirrors for ultrafast solid state lasers.